

# Supplement of “National CO<sub>2</sub> budgets (2015–2020) inferred from atmospheric CO<sub>2</sub> observations in support of the Global Stocktake”

Brendan Byrne<sup>1</sup>, David F. Baker<sup>2</sup>, Sourish Basu<sup>3,4</sup>, Michael Bertolacci<sup>5</sup>, Kevin W. Bowman<sup>1,6</sup>, Dustin Carroll<sup>7,1</sup>, Abhishek Chatterjee<sup>1</sup>, Frédéric Chevallier<sup>8</sup>, Philippe Ciais<sup>8</sup>, Noel Cressie<sup>5,1</sup>, David Crisp<sup>1</sup>, Sean Crowell<sup>9</sup>, Feng Deng<sup>10</sup>, Zhu Deng<sup>11</sup>, Nicholas M. Deutscher<sup>12</sup>, Manvendra K. Dubey<sup>13</sup>, Sha Feng<sup>14</sup>, Omaira E. García<sup>15</sup>, David W. T. Griffith<sup>12</sup>, Benedikt Herkommér<sup>16</sup>, Lei Hu<sup>17,18</sup>, Andrew R. Jacobson<sup>17,18</sup>, Rajesh Janardanan<sup>19</sup>, Sujong Jeong<sup>20</sup>, Matthew S. Johnson<sup>21</sup>, Dylan B. A. Jones<sup>10</sup>, Rigel Kivi<sup>22</sup>, Junjie Liu<sup>1,23</sup>, Zhiqiang Liu<sup>24</sup>, Shamil Maksyutov<sup>19</sup>, John B. Miller<sup>17</sup>, Scot M. Miller<sup>25</sup>, Isamu Morino<sup>19</sup>, Justus Notholt<sup>26</sup>, Tomohiro Oda<sup>27,28</sup>, Christopher W. O’Dell<sup>2</sup>, Young-Suk Oh<sup>29</sup>, Hirofumi Ohyama<sup>19</sup>, Prabir K. Patra<sup>30</sup>, Hélène Peiro<sup>9</sup>, Christof Petri<sup>26</sup>, Sajeev Philip<sup>31</sup>, David F. Pollard<sup>32</sup>, Benjamin Poulter<sup>3</sup>, Marine Remaud<sup>8</sup>, Andrew Schuh<sup>2</sup>, Mahesh K. Sha<sup>33</sup>, Kei Shiomi<sup>34</sup>, Kimberly Strong<sup>10</sup>, Colm Sweeney<sup>17</sup>, Yao Té<sup>35</sup>, Hanqin Tian<sup>36,37</sup>, Voltaire A. Velasco<sup>12,38</sup>, Mihalis Vrekoussis<sup>39,26</sup>, Thorsten Warneke<sup>26</sup>, John R. Worden<sup>1</sup>, Debra Wunch<sup>10</sup>, Yuanzhi Yao<sup>36</sup>, Jeongmin Yun<sup>20</sup>, Andrew Zammit-Mangion<sup>5</sup>, and Ning Zeng<sup>28,4</sup>

<sup>1</sup>Jet Propulsion Laboratory, California Institute of Technology, Pasadena, CA, USA

<sup>2</sup>Cooperative Institute for Research in the Atmosphere, Colorado State University, Fort Collins, CO, USA

<sup>3</sup>NASA Goddard Space Flight Center, Global Modeling and Assimilation Office, Greenbelt, MD, USA

<sup>4</sup>Earth System Science Interdisciplinary Center, College Park, MD, USA

<sup>5</sup>School of Mathematics and Applied Statistics, University of Wollongong, Australia

<sup>6</sup>Joint Institute for Regional Earth System Science and Engineering, University of California, Los Angeles, CA, USA

<sup>7</sup>Moss Landing Marine Laboratories, San José State University, Moss Landing, CA, USA

<sup>8</sup>Laboratoire des Sciences du Climat et de L’Environnement, LSCE/IPSL, CEA-CNRS-UVSQ, Université Paris-Saclay, 91191 Gif-sur-Yvette, France

<sup>9</sup>University of Oklahoma, Norman, OK, USA

<sup>10</sup>Department of Physics, University of Toronto, Toronto, Ontario, Canada

<sup>11</sup>Department of Earth System Science, Tsinghua University, Beijing, China

<sup>12</sup>Centre for Atmospheric Chemistry, School of Earth, Atmospheric and Life Sciences, University of Wollongong, Wollongong, NSW, Australia

<sup>13</sup>Earth System Observation, Los Alamos National Laboratory, Los Alamos, NM, USA

<sup>14</sup>Atmospheric Sciences and Global Change Division, Pacific Northwest National Laboratory, Richland, WA, USA

<sup>15</sup>Izaña Atmospheric Research Center (IARC), State Meteorological Agency of Spain (AEMet), Tenerife, Spain

<sup>16</sup>Institut for Meteorology and Climate Research (IMK-ASF), Karlsruhe Institute of Technology (KIT), Karlsruhe, Germany

<sup>17</sup>NOAA Global Monitoring Laboratory, Boulder, CO, USA

<sup>18</sup>Cooperative Institute for Research in Environmental Sciences, University of Colorado Boulder, Boulder, CO, USA

<sup>19</sup>Satellite Observation Center, Earth System Division, National Institute for Environmental Studies, Tsukuba, Japan

<sup>20</sup>Department of Environmental Planning, Graduate School of Environmental Studies, Seoul National University, Seoul, Republic of Korea

<sup>21</sup>NASA Ames Research Center, Moffett Field, CA, USA

<sup>22</sup>Space and Earth Observation Centre, Finnish Meteorological Institute, Sodankylä, Finland

<sup>23</sup>Division of Geological and Planetary Sciences, California Institute of Technology, Pasadena, CA, USA

<sup>24</sup>Laboratory of Numerical Modeling for Atmospheric Sciences & Geophysical Fluid Dynamics, Institute of Atmospheric Physics, Chinese Academy of Sciences, Beijing, China

- <sup>25</sup>Department of Environmental Health and Engineering, Johns Hopkins University, Baltimore, MD 21218, United States of America  
<sup>26</sup>Institute of Environmental Physics, University of Bremen, Bremen, Germany  
<sup>27</sup>Earth from Space Institute, Universities Space Research Association, Columbia, MD, USA  
<sup>28</sup>Department of Atmospheric and Oceanic Science, University of Maryland, USA  
<sup>29</sup>Global Atmosphere Watch Team, Climate Research Department, National Institute of Meteorological Sciences, Republic of Korea  
<sup>30</sup>Research Institute for Global Change, Japan Agency for Marine-Earth Science and Technology (JAMSTEC), Yokohama, 236-0001, Japan  
<sup>31</sup>Centre for Atmospheric Sciences, Indian Institute of Technology Delhi, New Delhi, India  
<sup>32</sup>National Institute of Water & Atmospheric Research Ltd (NIWA), Lauder, New Zealand  
<sup>33</sup>Royal Belgian Institute for Space Aeronomy (BIRA-IASB), Brussels, Belgium  
<sup>34</sup>Japan Aerospace Exploration Agency (JAXA), Tsukuba, Japan  
<sup>35</sup>Laboratoire d'Etudes du Rayonnement et de la Matière en Astrophysique et Atmosphères (LERMA-IPSL), Sorbonne Université, CNRS, Observatoire de Paris, PSL Université, 75005 Paris, France.  
<sup>36</sup>International Center for Climate and Global Change Research, College of Forestry, Wildlife and Environment, Auburn University, Auburn, AL 36849, USA  
<sup>37</sup>Schiller Institute for Integrated Science and Society, and Department of Earth and Environmental Sciences, Boston College, Chestnut Hill, MA 02467, USA  
<sup>38</sup>Deutscher Wetterdienst (DWD), Hohenpeissenberg, Germany.  
<sup>39</sup>Climate and Atmosphere Research Center (CARE-C), The Cyprus Institute, Nicosia, Cyprus

**Correspondence:** Brendan Byrne (brendan.k.byrne@jpl.nasa.gov)

*Copyright statement.* ©2022. California Institute of Technology, government sponsorship acknowledged.

## 1 Introduction

This supporting information contains one text section listing the countries within the regional groupings, and 12 supplementary figures.

5

### Text S1. Regional groupings

- **ASEAN:** Brunei, Cambodia, Indonesia, Laos, Malaysia, Mayanmar, Philippines, Singapore, Thailand, Vietnam
- **African Union (AU):** Algeria, Angola, Benin, Botswana, Burkina Faso, Burundi, Cameroon, Central African Republic, Chad, Comoros, Democratic Republic of Congo, Djibouti, Egypt, Equatorial Guinea, Eritrea, Eswatini, Ethiopia, Gabon, The Gambia, Ghana, Guinea, Guinea-Bissau, Ivory Coast, Kenya, Lesotho, Liberia, Libya, Madagascar, Malawi, Mali, Mauritania, Mauritius, Morocco, Mozambique, Namibia, Niger, Nigeria, The Congo, Rwanda, Western Sahara, Sao Tome and Principe, Senegal, Seychelles, Sierra Leone, Somalia, South Africa, South Sudan, Sudan, Tanzania, Togo, Tunisia, Uganda, Zambia, Zimbabwe

10

- **AU North:** Algeria, Egypt, Libya, Mauritania, Morocco, Western Sahara, Tunisia
- 15 – **AU South:** Angola, Botswana, Eswatini, Lesotho, Malawi, Mozambique, Namibia, South Africa, Zambia, Zimbabwe
- **AU West:** Benin, Burkina Faso, The Gambia, Ghana, Guinea, Guinea-Bissau, Ivory Coast, Liberia, Mali, Niger, Nigeria, Senegal, Sierra Leone, Togo
- **AU East:** Comoros, Djibouti, Eritrea, Ethiopia, Kenya, Madagascar, Mauritius, Rwanda, Seychelles, Somalia, South Sudan, Sudan, Tanzania, Uganda
- 20 – **AU Central:** Burundi, Cameroon, Central African Republic, Chad, Democratic Republic of Congo, Equatorial Guinea, Gabon, The Congo
- **CELAC+Brazil:** Antigua and Barbuda, Argentina, Bahamas, Belize, Bolivia, Chile, Columbia, Costa Rica, Cuba, Dominica, Dominican Republic, Ecuador, El Salvador, Grenada, Guatemala, Guyana, Haiti, Honduras, Jamaica, Mexico, Nicaragua, Panama, Paraguay, Peru, Saint Kitts and Nevis, Saint Lucia, Saint Vincent and Grenadines, Suriname, Trinidad and Tobago, Uruguay, Venezuela, Brazil
- **ECO:** Afghanistan, Azerbaijan, Iran, Kazakhstan, Kyrgyzstan, Pakistan, Tajikistan, Turkey, Turkmenistan, Uzbekistan
- **European Union (EU):** Austria, Belgium, Bulgaria, Croatia, Cyprus, Czech Republic, Denmark, Estonia, Finland, France, Germany, Greece, Hungary, Ireland, Italy, Latvia, Lithuania, Luxembourg, Malta, Netherlands, Poland, Portugal, Romania, Slovakia, Slovenia, Spain, Sweden
- 30 – **SAARC:** Afghanistan, Bangladesh, Bhutan, India, Maldives, Nepal, Pakistan, Sri Lanka
- **North America:** Canada, USA, Mexico
- **Middle East:** Bahrain, Cyprus, Egypt, Iran, Iraq, Israel, Jordan, Kuwait, Lebanon, Oman, Palestine, Qatar, Saudi Arabia, Syria, Turkey, United Arab Emirates, Yemen
- **Europe:** Albania, Andorra, Austria, Belarus, Belgium, Bosnia and Herzegovina, Bulgaria, Croatia, Czech Republic, Denmark, Estonia, Finland, France, Germany, Greece, Hungary, Iceland, Ireland, Italy, Latvia, Liechtenstein, Lithuania, Luxembourg, Malta, Moldova, Monaco, Montenegro, Netherlands, North Macedonia, Norway, Poland, Portugal, Romania, San Marino, Serbia, Slovakia, Slovenia, Spain, Sweden, Switzerland, Ukraine, United Kingdom, The Vatican

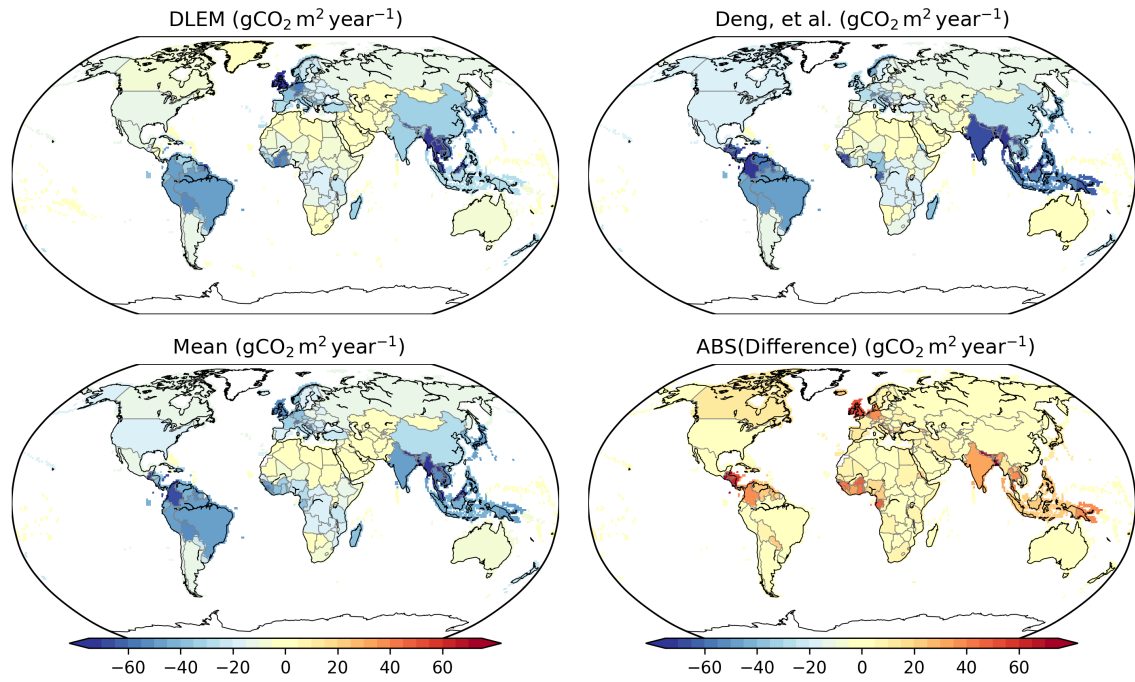


**Figure S1.** 2015–2020 mean  $F_{\text{rivers export}}$  for countries estimated by (top-left) the DLEM model, (top-right) Deng et al. (2022), (bottom-left) mean of these two estimates, and (bottom-right) the absolute difference between these two estimates

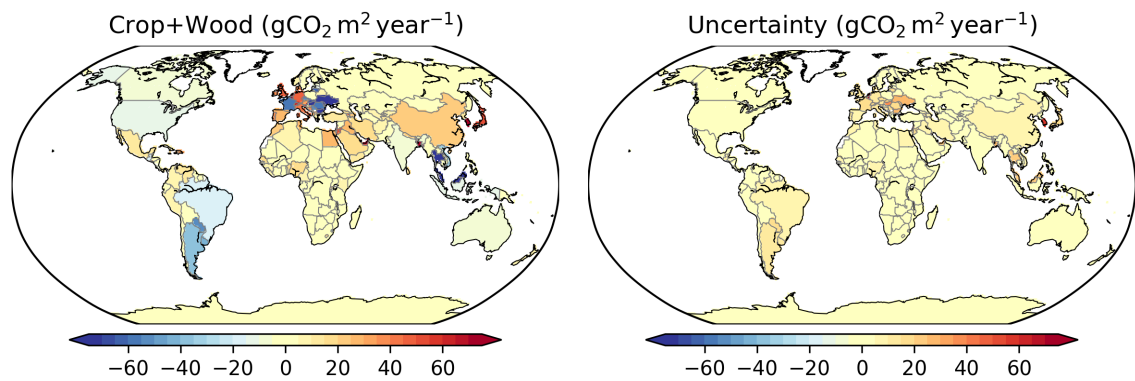


**Figure S2.** 2015–2019 mean  $F_{\text{crop trade}} + F_{\text{wood trade}}$  and their uncertainty (assumed to be a 30% of the flux).

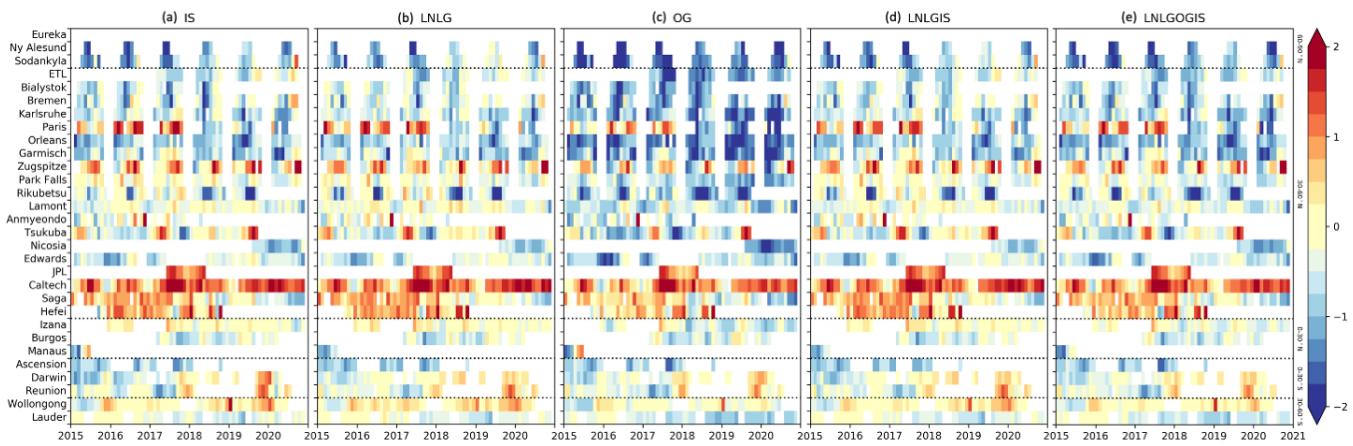


**Figure S3.** Monthly mean difference between retrieved and simulated  $X_{CO_2}$  for the v10 OCO-2 MIP median model (data minus model) at each TCCON site. Biases are shown for each experiment: (a) IS, (b) LNLG, (c) OG, (d) LNLGIS, and (e) LNLGOGIS. Dashed black lines demarcate  $30^\circ$  latitude bounds.

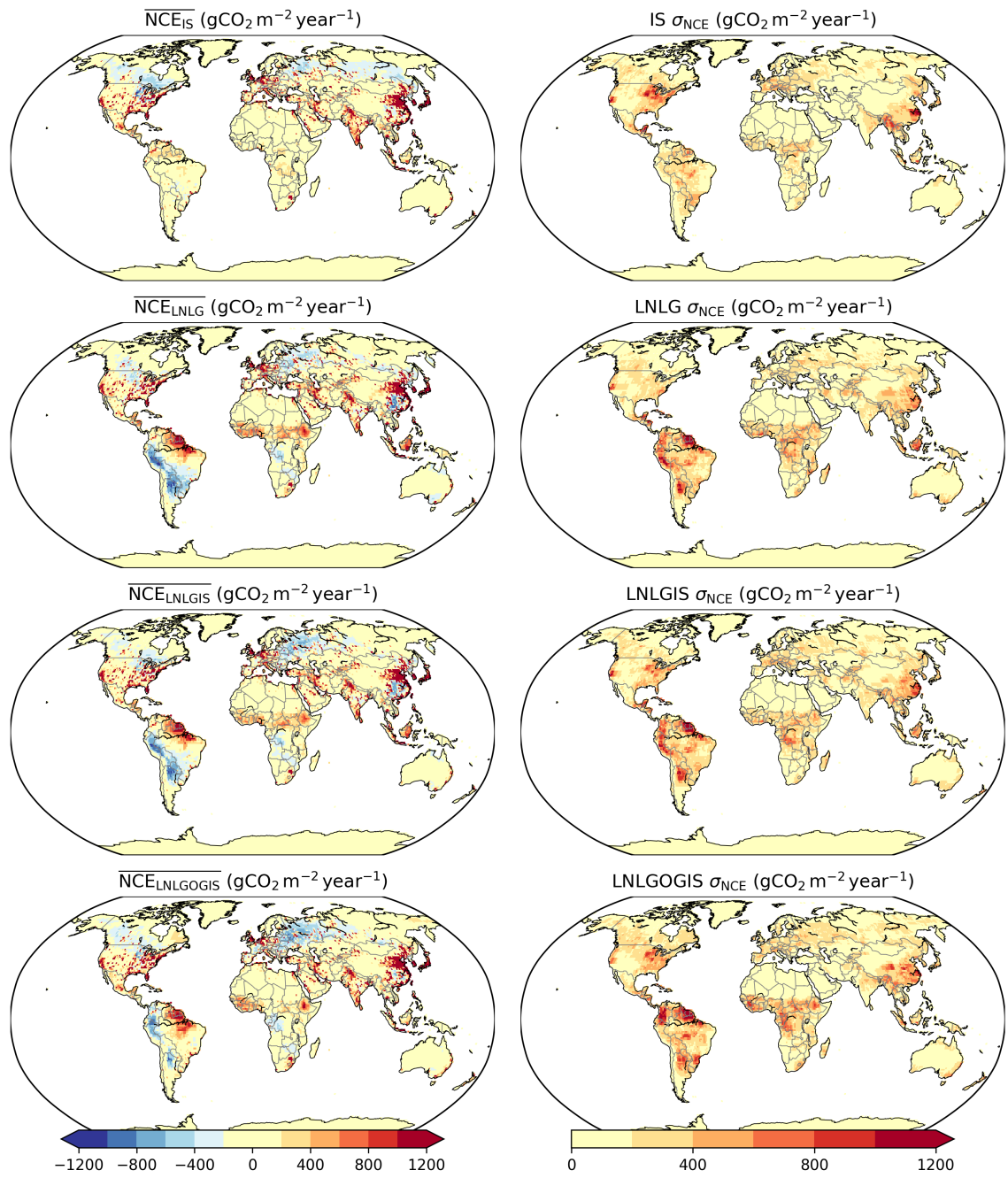


**Figure S4.**  $1^\circ \times 1^\circ$  grid median and standard deviation of  $\text{NCE}$  ( $\text{gCO}_2 \text{ m}^{-2} \text{ yr}^{-1}$ ) over 2015–2020 from the v10 OCO-2 MIP for the (1st row) IS, (2nd row) LNLG, (3rd row) LNLGIS and (4th row) LNLGOGIS experiments.

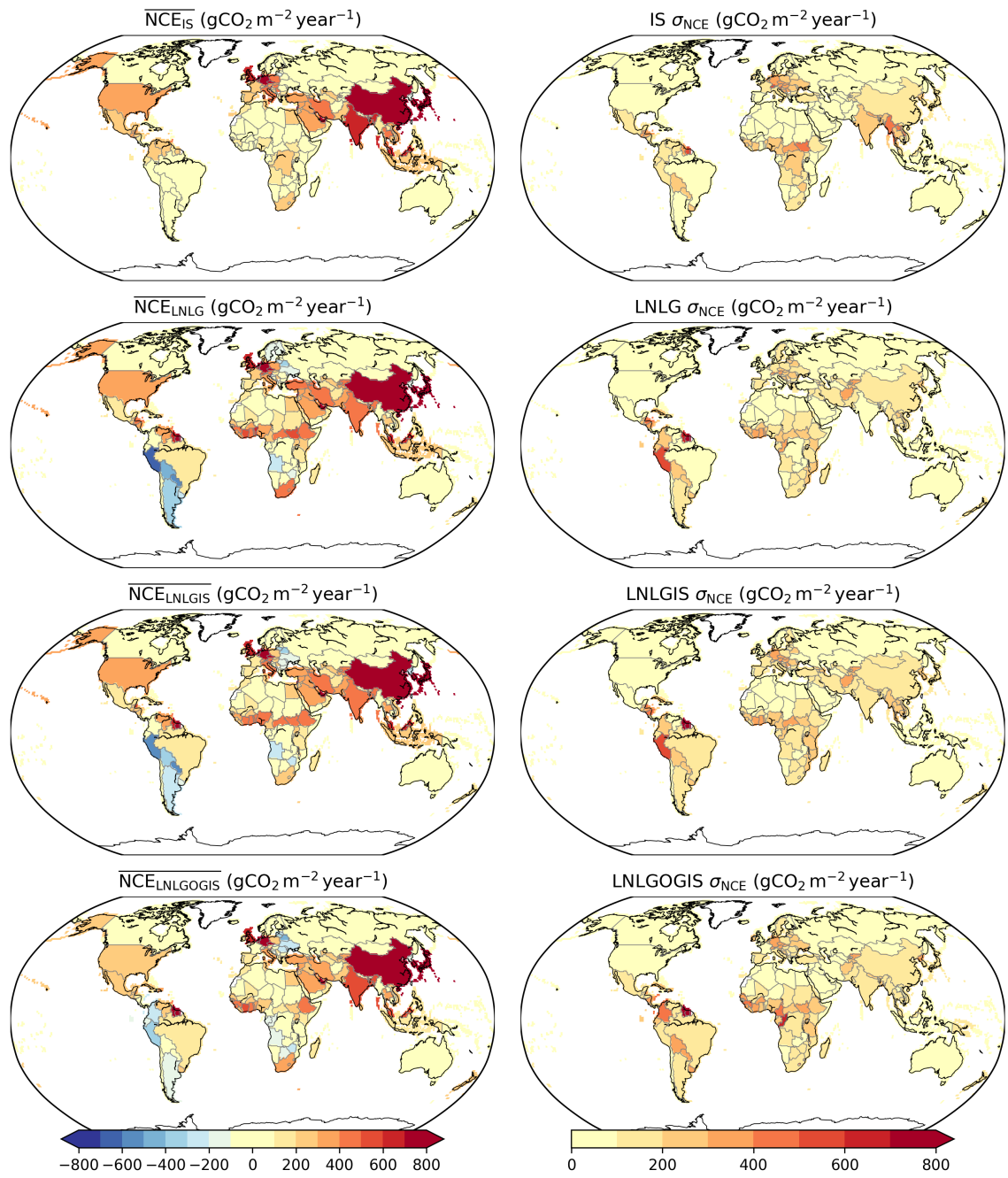


**Figure S5.** Country level median and standard deviation of NCE ( $\text{gCO}_2 \text{ m}^{-2} \text{ yr}^{-1}$ ) over 2015-2020 from the v10 OCO-2 MIP for the (1st row) IS, (2nd row) LNLG, (3rd row) LNLGIS and (4th row) LNLGOGIS experiments.

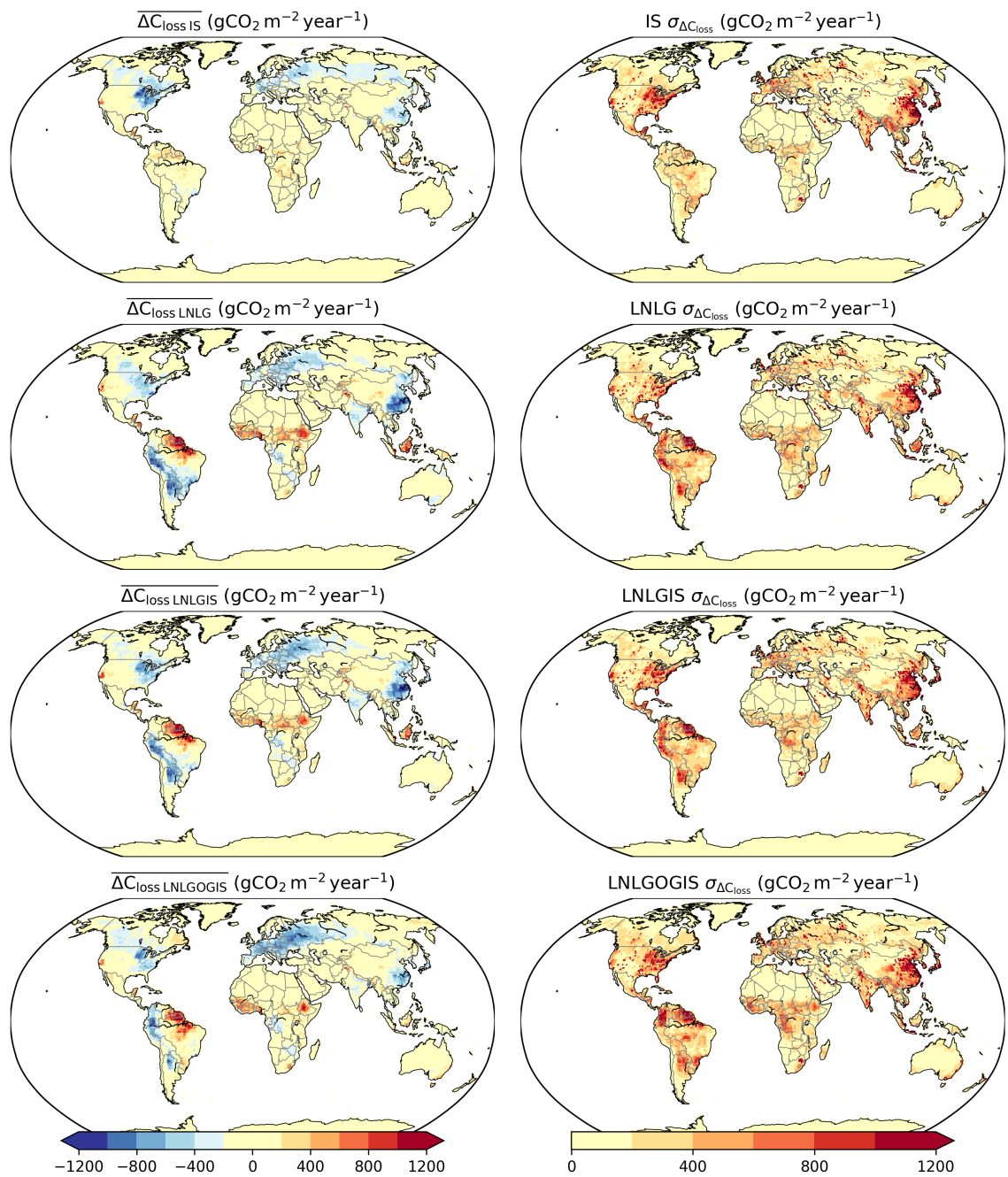


**Figure S6.** 2015–2020 mean annual net  $\Delta C_{\text{loss}}$  ( $\text{gCO}_2 \text{m}^{-2} \text{yr}^{-1}$ ), and their uncertainties.

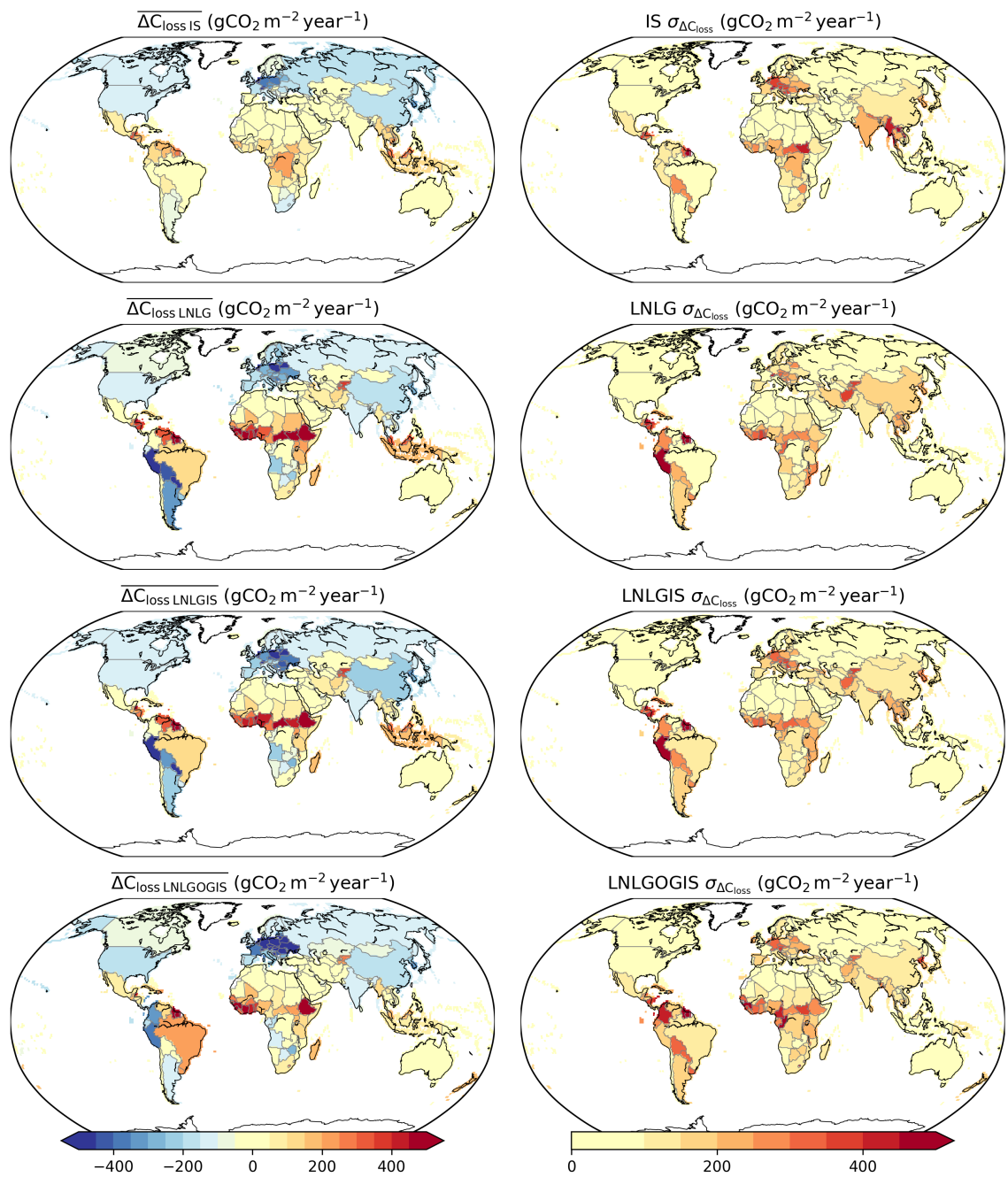


**Figure S7.** 2015–2020 mean annual net  $\Delta C_{\text{loss}}$  ( $\text{gCO}_2 \text{ m}^{-2} \text{ yr}^{-1}$ ) and their uncertainties.

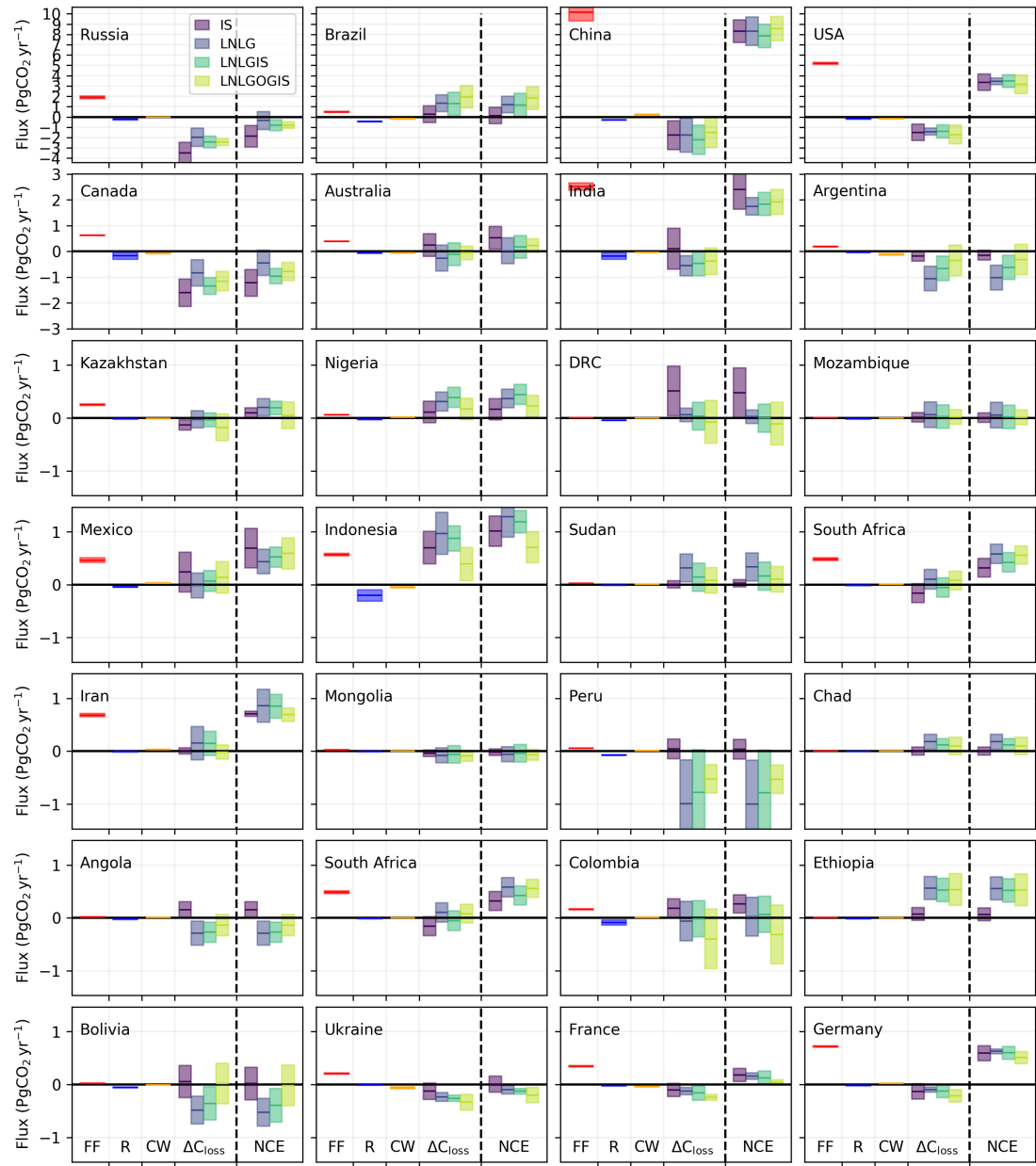


**Figure S8.** Bar plot of 2015–2020 median +/- standard deviation of FF,  $F_{\text{rivers export}}$  (R),  $F_{\text{crop trade}}+F_{\text{wood trade}}$  (CW),  $\Delta C_{\text{loss}}$ , and NCE for 28 countries. Note that different rows have different y-axis limits.

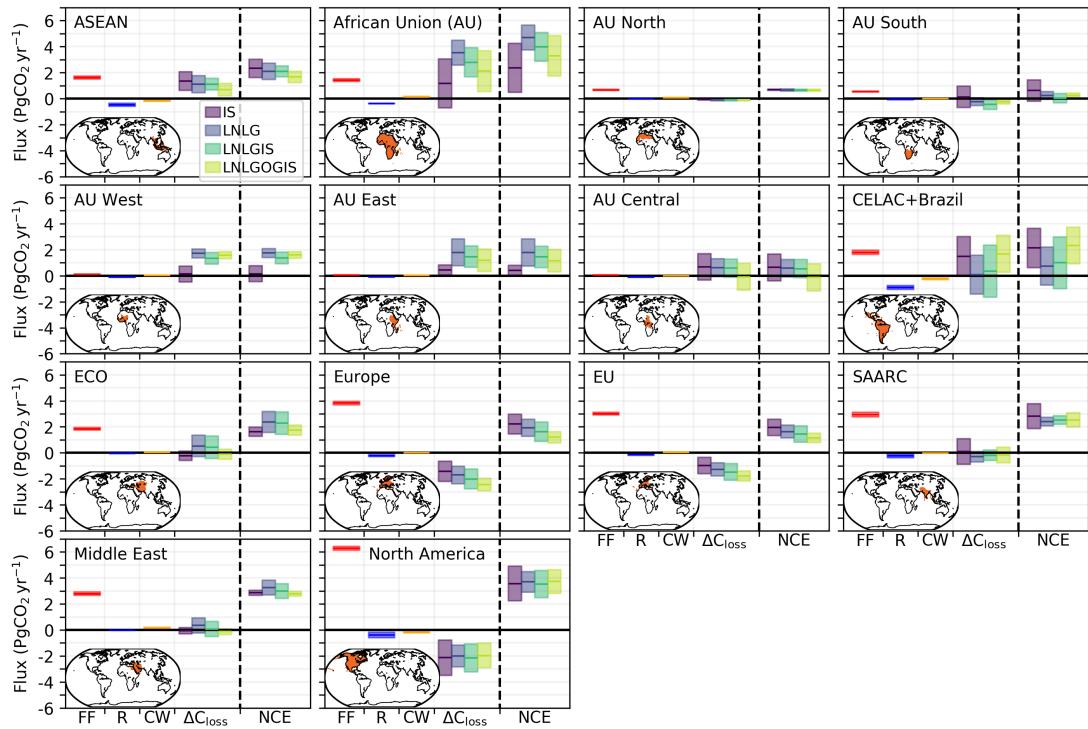


**Figure S9.** Bar plot of 2015–2020 median +/- standard deviation of FF,  $F_{\text{rivers export}}$  (R),  $F_{\text{crop trade}} + F_{\text{wood trade}}$  (CW),  $\Delta C_{\text{loss}}$ , and NCE for 14 regions composed of multiple countries.

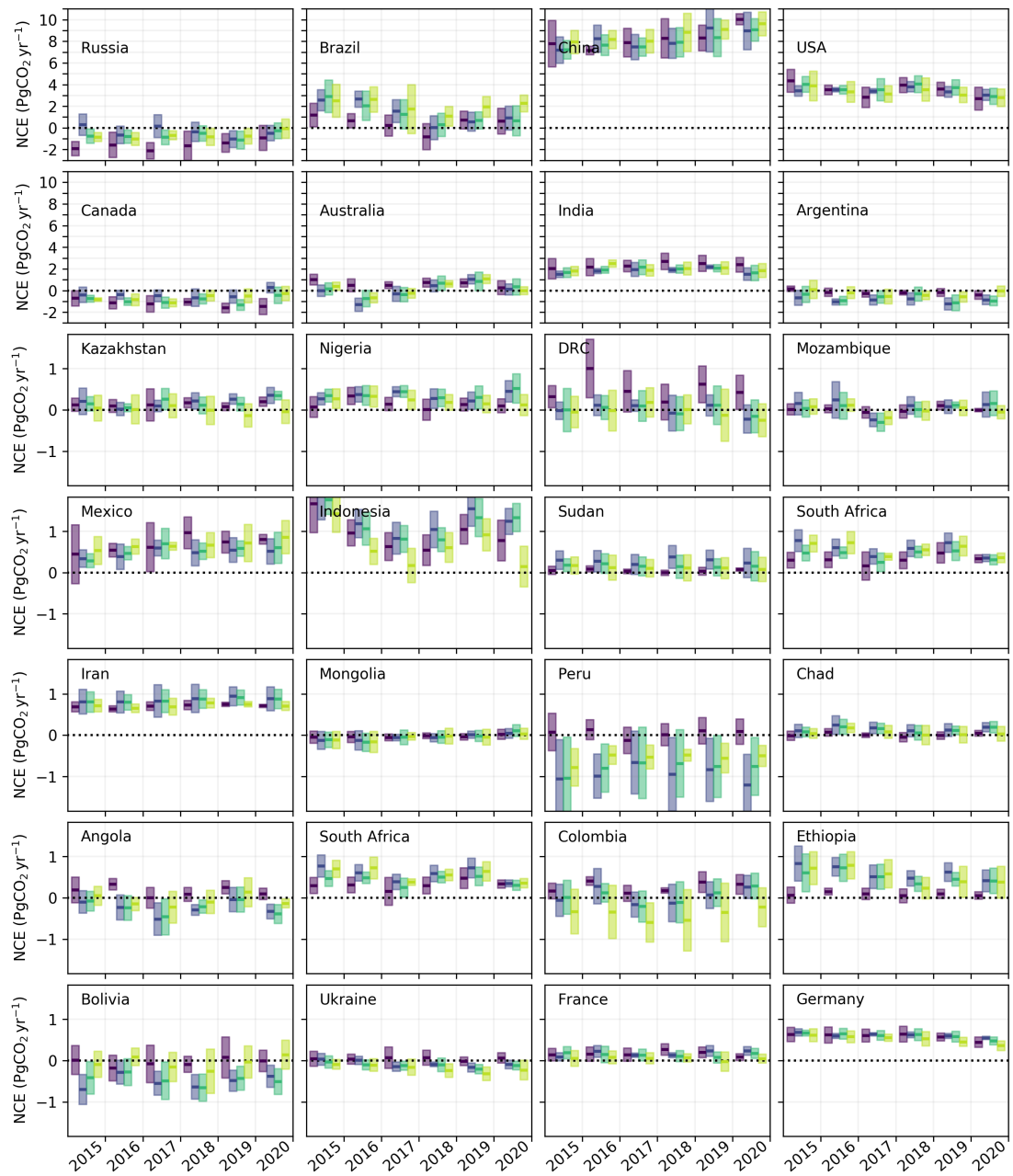


**Figure S10.** Timeseries of NCE for 28 countries (median +/- standard deviation) for the IS, LNLG, LNLGIS, and LNLGOGIS inversions.

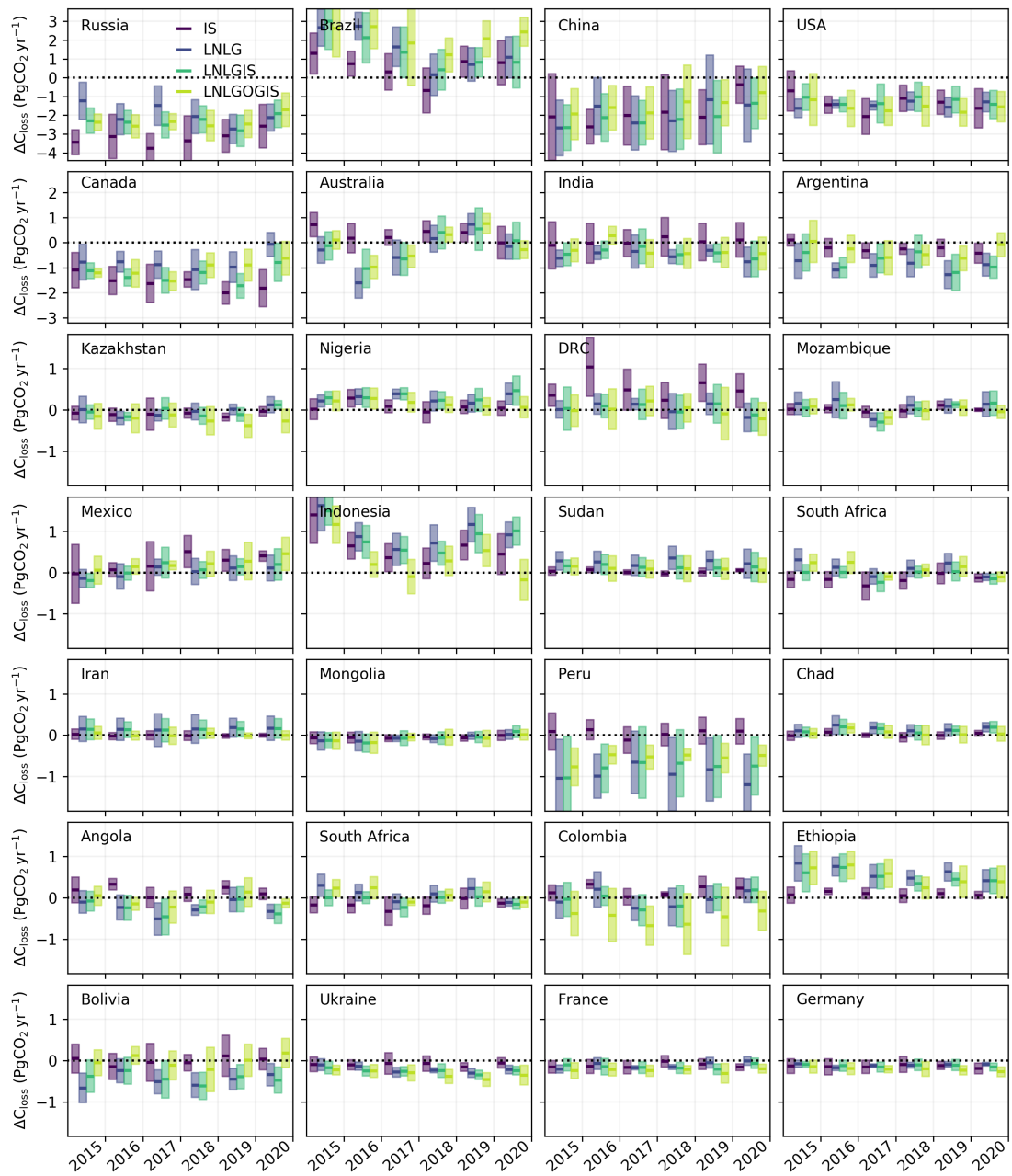


**Figure S11.** Timeseries of  $\Delta C_{\text{loss}}$  for 28 countries (median +/- standard deviation) for the IS, LNLG, LNLGIS, and LNLGOGIS inversions.

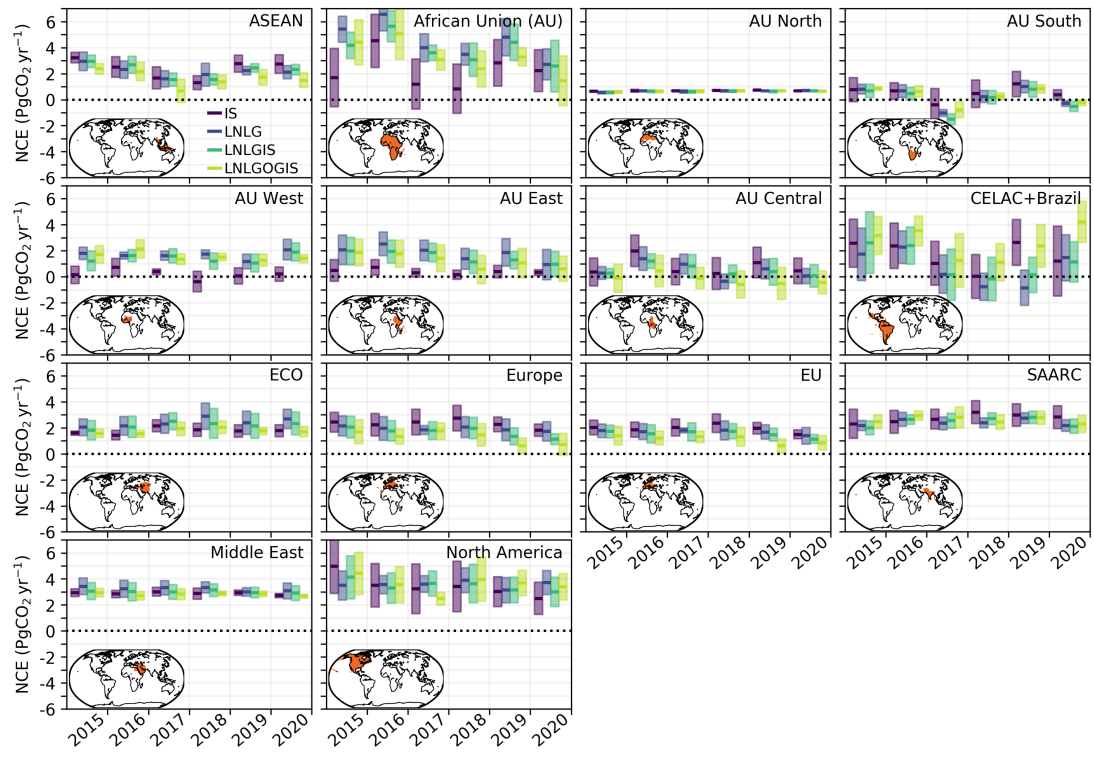


**Figure S12.** Timeseries of NCE for 14 regions composed of multiple countries (median +/- standard deviation) for the IS, LNLG, LNLGIS, and LNLGOGIS inversions.

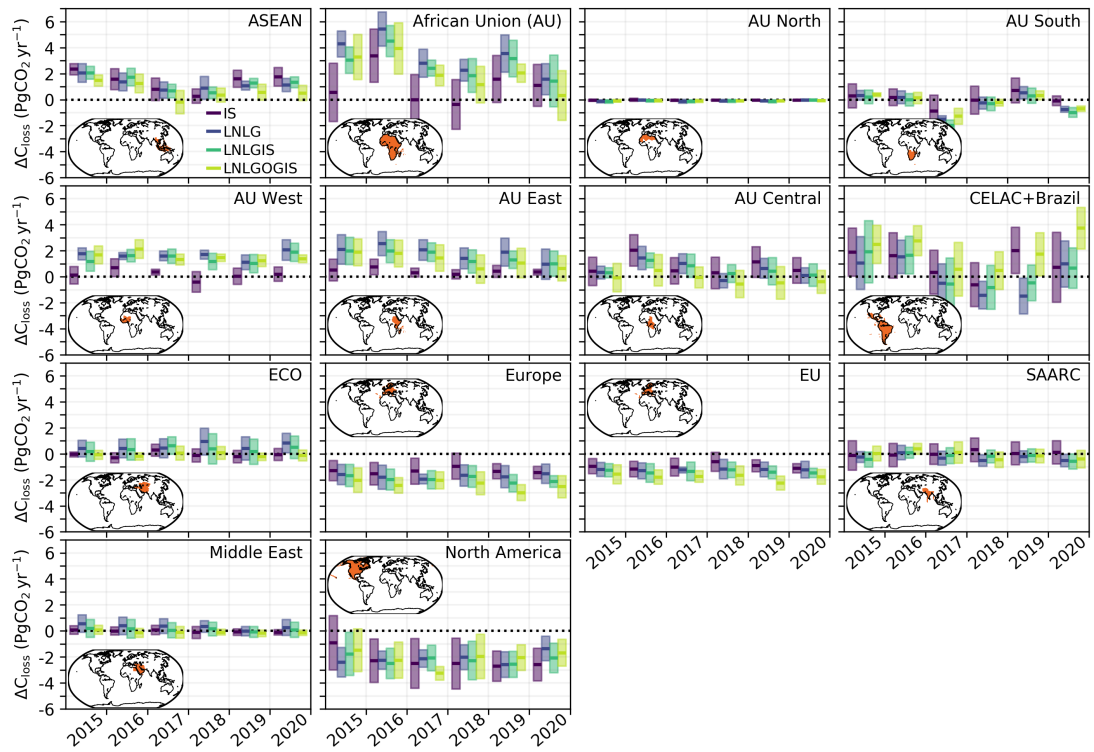


**Figure S13.** Timeseries of  $\Delta C_{\text{loss}}$  for 14 regions composed of multiple countries (median +/- standard deviation) for the IS, LNLG, LNLGIS, and LNLGOGIS inversions.

## References

- Deng, Z., Ciais, P., Tzompa-Sosa, Z. A., Saunois, M., Qiu, C., Tan, C., Sun, T., Ke, P., Cui, Y., Tanaka, K., Lin, X., Thompson, R. L., Tian,  
40 H., Yao, Y., Huang, Y., Lauerwald, R., Jain, A. K., Xu, X., Bastos, A., Sitch, S., Palmer, P. I., Lauvaux, T., d'Aspremont, A., Giron, C.,  
Benoit, A., Poulter, B., Chang, J., Petrescu, A. M. R., Davis, S. J., Liu, Z., Grassi, G., Albergel, C., Tubiello, F. N., Perugini, L., Peters, W.,  
and Chevallier, F.: Comparing national greenhouse gas budgets reported in UNFCCC inventories against atmospheric inversions, *Earth  
Syst. Sci. Data*, 14, 1639–1675, <https://doi.org/10.5194/essd-14-1639-2022>, 2022.